ORNL/TM-2017/723

SPECIES-SPECIFIC SUSCEPTIBILITY TO SCALE LOSS: USING SIMULATED SHEAR TO UNDERSTAND AMONG SPECIES DIFFERENCES IN TURBINE PASSAGE INJURY

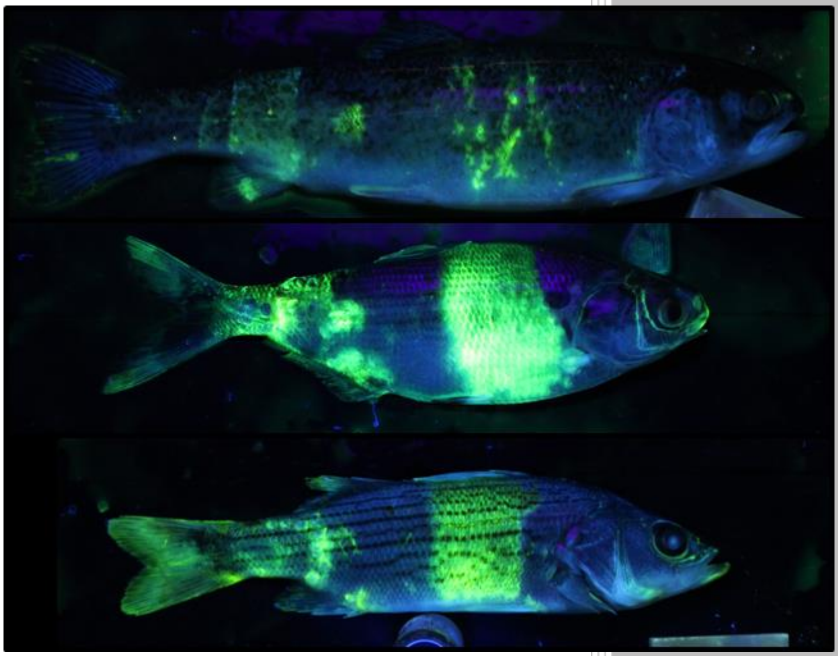

R. K. Saylor
M. S. Bevelhimer
A. M. Fortner
B. M. Pracheil

December 2017

OAK RIDGE NATIONAL LABORATORY
MANAGED BY UT-BATTELLE FOR THE US DEPARTMENT OF ENERGY

ORNL/TM-2017/723

Environmental Sciences Division

SPECIES-SPECIFIC SUSCEPTIBILITY TO SCALE LOSS: USING SIMULATED SHEAR TO UNDERSTAND AMONG SPECIES DIFFERENCES IN TURBINE PASSAGE INJURY

R. K. Saylor
M. S. Bevelhimer
A. M. Fortner
B. M. Pracheil

December 2017

Prepared by
OAK RIDGE NATIONAL LABORATORY
Oak Ridge, TN 37831-6283
managed by
UT-BATTELLE, LLC
for the
US DEPARTMENT OF ENERGY
under contract DE-AC05-00OR22725

CONTENTS

LIST OF FIGURES

LIST OF TABLES

ACRONYMS

ANOVA	Analysis of Variance
BioDE	Biologically-based Design and Evaluation
BioPA	Biological Performance Assessment
GZS	Gizzard Shad
HSB	Hybrid Striped Bass
ISO	International Organization of Standardization
ORNL	Oak Ridge National Laboratory
PNNL	Pacific Northwest National Laboratory
RBT	Rainbow Trout
SERD	Shear Exposure Restraining Device
TEA	Targeted Exposure Area
USEIA	U.S. Energy Information Administration
UV	Ultraviolet

1. INTRODUCTION

Hydropower is the largest source of utility-scale, renewable electricity (e.g., 44% of all renewable energy) in the USA to date (U.S. Energy Information Administration (USEIA), 2017); however, dam installation and operation have impacted natural upstream and downstream fish passage and altered connectivity of riverine fish communities throughout the USA (Čada, 1998; Čada et al., 2006; Pracheil et al., 2016a). Fish ladders and exclusion devices (among others) allow fish to safely circumvent and avoid passage through the turbines altogether (Čada, 2001), but are rarely 100% effective. At many dams, passage through turbines is unavoidable, and stressors like collision with structures or blade strike, barotrauma or cavitation, turbulence, and exposure to shear forces may cause injury or mortality to entrained fish (Čada, 2001; Neitzel et al., 2004; Pracheil et al., 2016a). Passage injury and mortality may be a consequence of exposure to the entire suite of stressors, while the exact role of each is difficult to ascertain and link to individuals (Colotelo et al., 2017). Contributing complicating factors to understanding mortality include turbine type, variation in fish size (i.e., life stages), and the marked morphological diversity of freshwater fishes (Pracheil et al., 2016a; Colotelo et al., 2017). Laboratory studies aimed to understand the effects of turbine passage have quantified each stressor separately to determine appropriate dose-response relationships based on fish size, species, etc. Establishing dose-response relationships by stressor for priority species that interact with hydropower dams is one of the primary objectives of the Biologically-based Design and Evaluation (BioDE) project being conducted at Oak Ridge National Laboratory (ORNL) and Pacific Northwest National Laboratory (PNNL). At its core, BioDE is focused on empirically driven research that quantifies fish responses to stressors at exposure levels similar to those experienced during turbine passage so that Biological Performance Assessment (BioPA) models can be developed. The BioPA model informs hydropower turbine design modifications based on predicted injury and mortality in response to various stressor exposures, e.g., blade strike, shear, and barotrauma. Stress exposure is defined by computational fluid dynamics models of the turbine environment. Fish response relationships are determined through laboratory studies like the one reported in this document. The BioPA model will aid turbine manufactures, plant operators, and dam owners with design of lower impact turbines and modify operating procedures to maximize survival of entrained fishes.

A variety of injuries have been associated with turbine passage, and one of the most common is scale loss of varying degrees (Normandeau et al., 1996). Loss of some scales is not uncommon naturally, such as during an attack by a predator, and scale replacement often occurs. However, more substantial scale loss has been linked to overall poor physiological condition (Basham et al., 1982) and increased mortality (Kostecki et al., 1987). Laboratory studies were unable to link mortality to scale loss over 48 hours (Kostecki et al., 1987), whereas 7 day mortality was observed as a result of scale loss (Turnpenny, 1998) and common injuries in laboratory shear studies were cited as scale loss (Deng et al., 2005; van Esch et al., 2014). Latent mortality from increased disease susceptibility (Turnpenny, 1998; Hostetter et al., 2011), ionic and osmotic stress (Kostecki et al., 1987), or increased predation (Neitzel et al., 2000) may also be linked to scale loss caused by shear exposure. Hydraulic shear occurs at the intersecting layer between two masses of water moving at different velocities or as one interacts with a solid structure (Čada, 2001; Čada et al., 2006). Shear exposure (magnitude and duration) within a turbine depends on flow rate among other things, with the most severe probability of shear injury occurring in Francis turbines as water enters through the stay vanes and wicket gates, interacts with the runner, and exits into the draft tube towards the tailrace (Čada et al., 2006).

Although several reports provide ample evidence of shear forces inducing scale loss in fish, generalizations across a wide range of species is difficult because only a small number of species have been investigated to date. Recent laboratory studies have shown that descaling is species dependent (Neitzel et al., 2004). Field studies provide the most realistic turbine passage response data but have little to no ability to quantify the exact exposure that individual fish experience. Laboratory studies are less realistic than field studies but have greater control during exposure protocols (Figure 1); however, there is still variation in injury and mortality estimates caused by less precise control over dosage level. The lack of scale loss data for more than just a few species decreases the overall inference space of the BioPA model. A larger data base that accounts for the marked integumental diversity (e.g., scale type, size, shape, skin thickness, etc.) among fishes would provide the foundation for predicting potential descaling and related injuries for a wide range of species as a result of turbine passage.

The experimental objective of this study was to expose fishes to a high velocity jet of water to quantify descaling susceptibility among adult fishes. Our ultimate objective was to create dose-response curves of scale loss after exposure to different doses of shear. The BioDE studies conducted in Fiscal Year 2016 by ORNL were designed at the most basic level to assess susceptibility of a variety of fish types to descaling and other external injuries when exposed to tightly controlled and defined shear exposure. In keeping with the traits-based approach from previous analyses (Čada & Schweizer, 2012; Pracheil et al., 2016b), we conducted studies on species that represent a range of integument types so that we could develop a broad inference space within which turbine passage effects (e.g., descaling) can be predicted or assessed for these and similar species.

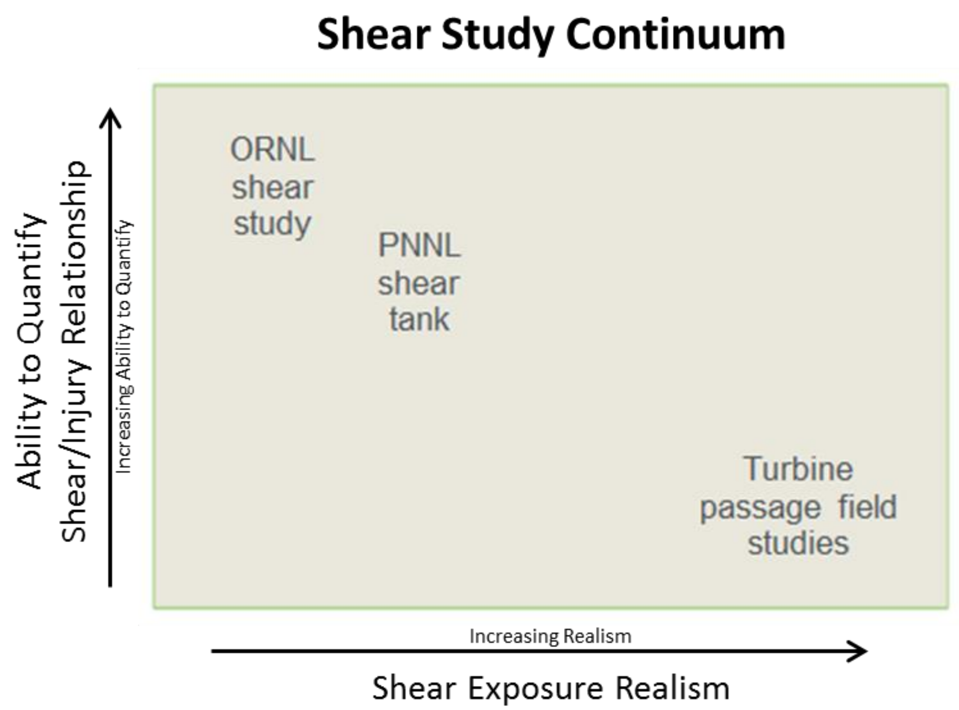

Figure 1. The diagram above is a representation of the shear study continuum to better delineate how prior studies fit within its framework. More specifically, it visually displays how studies (past and presented in this report) have addressed realism and the ability to quantify shear injury relationships (i.e., control of dosage in order to predict a response).

2. MATERIALS AND METHODS

Experimental Design

Shear Exposure Apparatus – We designed an experimental apparatus that could repeatedly subject fish to a measurable dose of simulated shear force. Two submersible pumps (rated maximum flow rate of 3.93 × 10-3 and 8.08 × 10-3 m3/s) were plumbed in tandem so that water passed through ~ 1 m of pipe that gradually stepped down in diameter from 5.1 to 1.9 cm (Figure 2). The latter maximized dosage velocity delivered to individual fish as it was passed through the exposure nozzle. The nozzle consisted of a 20 cm copper pipe ending with a 5 × 25 mm oblong opening and a cross-sectional area of ~145 mm2. We used volumetric flow rate to estimate flow rate and calculate velocity of our system. Fill times (s) of a container with volume of 0.084 m3 were estimated in triplicate when the gate valve was one-quarter, halfway, or fully open (1, 2, or 3.83 revolutions, respectively). The maximum flow rate of our system was estimated to be 1.60 × 10-3 m3/s, which resulted in a calculated maximum velocity at the nozzle of 11.0 m/s. Exposure velocity was regulated using a 2.5 cm gate valve located immediately prior to the copper nozzle. Exposure time was controlled by connecting the pump's power supplies to an electronic timer that limited water jet exposure to 1.5 s. Experiments were performed in a 6.4 m long, 0.3 m wide, 0.3 m deep oval raceway that minimized turbulence resulting from the water jet contacting the sides or bottom of the tank.

Figure 2. The image above depicts our simulated shear exposure apparatus used to generate exposure velocities (dose) and estimate descaling rates (response) in fishes. Water was pumped through two submersible pumps (maximum rated flow of 3.93 × 10-3 [1] and 8.08 × 10-3 [2] m3/s) and a gate valve (3) was used to control the water jet exiting the nozzle (4; inset picture). Water exiting the nozzle interacted with fish that were secured to the submerged shear platform (5; inset picture).

Shear exposure restraining device (SERD) – Euthanized fish were exposed to the water jet by securing each to an underwater platform composed of a weighted, epoxy-coated wire shelf to maintain dosage consistency. The SERD was comprised of a fish transfixed through the mouth with a metal prod, which was secured to a plastic plank using a 0.5 cm Velcro strap and 1.6 cm wingnut. The SERD was attached to the underwater platform so that the head was oriented downstream (i.e., in line) with water flow (Figure 3). Height of the SERD was adjusted to accommodate variation in girth to maintain a 1 cm exposure distance between the nozzle tip and body surface. The nozzle tip was secured at a 45° angle to that of the fish's body surface. Exposure distance and nozzle angle also ensured the water jet would interact with the margins of exposed scales. Combined, our method allowed us to consistently expose fish to simulated shear velocity by accounting for individual and species-related variation in body shape.

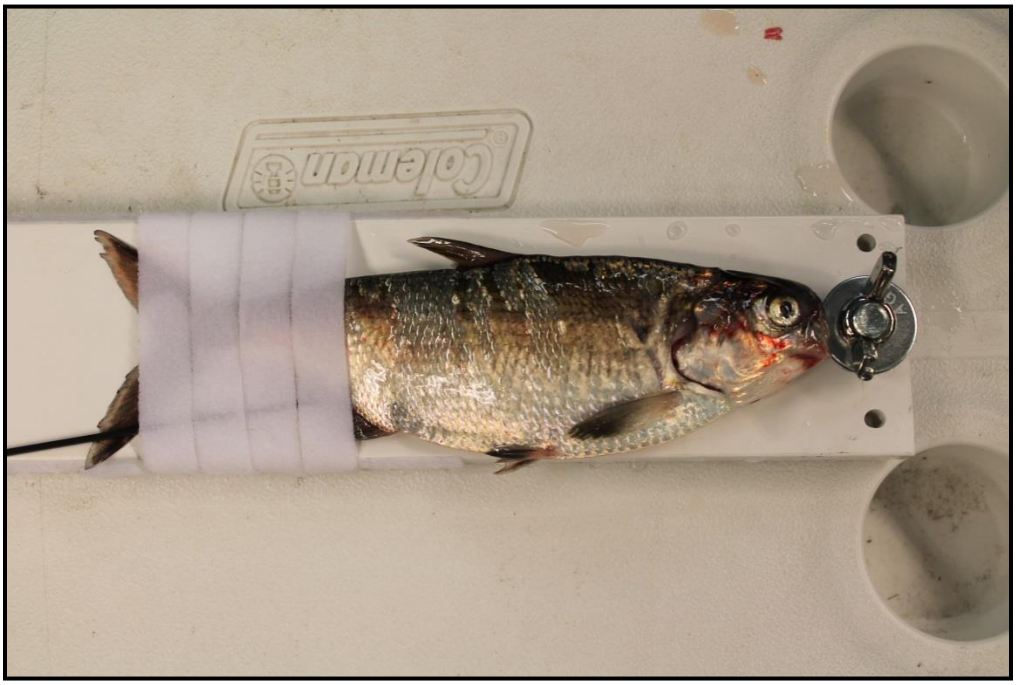

Figure 3. A gizzard shad positioned on the shear exposure restraining device (SERD) with wing nut (W) and Velcro (V) holding straps securing the transfixed (T) fish to the base (B) for simulated shear exposure. NOTE: the X's show two areas of scale loss and the arrow indicates direction of water flow.

Species – Our experiment was designed to investigate how fish integument responds to shear stress by including a variety of species that vary by scale type and size. We used three species: rainbow trout (Oncorhynchus mykiss; total length [TL] 20.8 – 31.3 cm), gizzard shad (Dorosoma cepedianum; TL 17.0 – 29.0 cm), and hybrid striped bass (striped bass [Morone saxatilus] × white bass [M. chrysops]; TL 16.3 – 24.0 cm). Rainbow trout and gizzard shad were purchased from a local state hatchery and bait shop in Tennessee, respectively, and hybrid striped based were purchased from a private hatchery in Arkansas. Rainbow trout were chosen as a representative of anadromous Ssalmonids which often experience turbine passage throughout North America, but most notably in the Pacific Northwest. Gizzard shad represent the Cclupeid family of fishes that interact with hydropower projects found within inland and coastal rivers, primarily in the northeast US. Hybrid striped bass were chosen to represent the Moronid family containing species that routinely migrate through Atlantic Coast rivers containing hydropower dams. Fish were maintained in round, 680-L fiberglass tanks with constant flow of freshwater and aeration. Trials were commenced, and generally completed, within 72 hours of fish arriving at the laboratory.

Exposure Velocities – The exposure velocities ranged from 0 (control) to 11.0 m/s (maximum available velocity for our set-up), but varied slightly according to species. Pilot studies indicated that maximum exposure velocity was needed for complete removal of rainbow trout scales but not for gizzard shad or hybrid striped bass. A total of four treatment exposure velocities were chosen for each species based on preliminary testing to identify at what velocities descaling was near 0 and 100%. Rainbow trout were exposed to 0, 5.0, 8.0, and 11.0 m/s, whereas both gizzard shad and hybrid striped bass were exposed to 0, 4.1, 5.9, and 7.3 m/s. Actual exposure velocities were set based on the relationship between gate valve revolutions (i.e., percentage open) and calculated velocity. Use of different velocities was necessary to generate more accurate dose response relationships across species. We used 30 fish for each exposure velocity (i.e., n = 120 total for each species) which allowed us to increase species coverage of descaling rate estimates. Our methodology used fewer individuals per exposure treatment but included more species in descaling estimates, thereby increasing the inference space of the BioPA model framework parameterized with these data.

Exposure Site – Fish were positioned on the SERD and underwater platform such that the approximate exposure area for every individual across all species was consistent. More specifically, the body surface between the midpoint of the dorsal fin to the margin of the operculum became the targeted exposure area (TEA), (Figure 4). Consistent alignment within species was maintained by aligning the nozzle with 1) the leading edge of the pelvic fin in rainbow trout, 2) the trailing edge of pelvic fin in gizzard shad, and 3) the trailing edge of the spiny dorsal fin in hybrid striped bass. A 35 × 35 mm (width × length) with an approximate surface area of 1225 mm2 was placed inside the TEA of each species to estimate proportional descaling loss during post hoc image analyses.

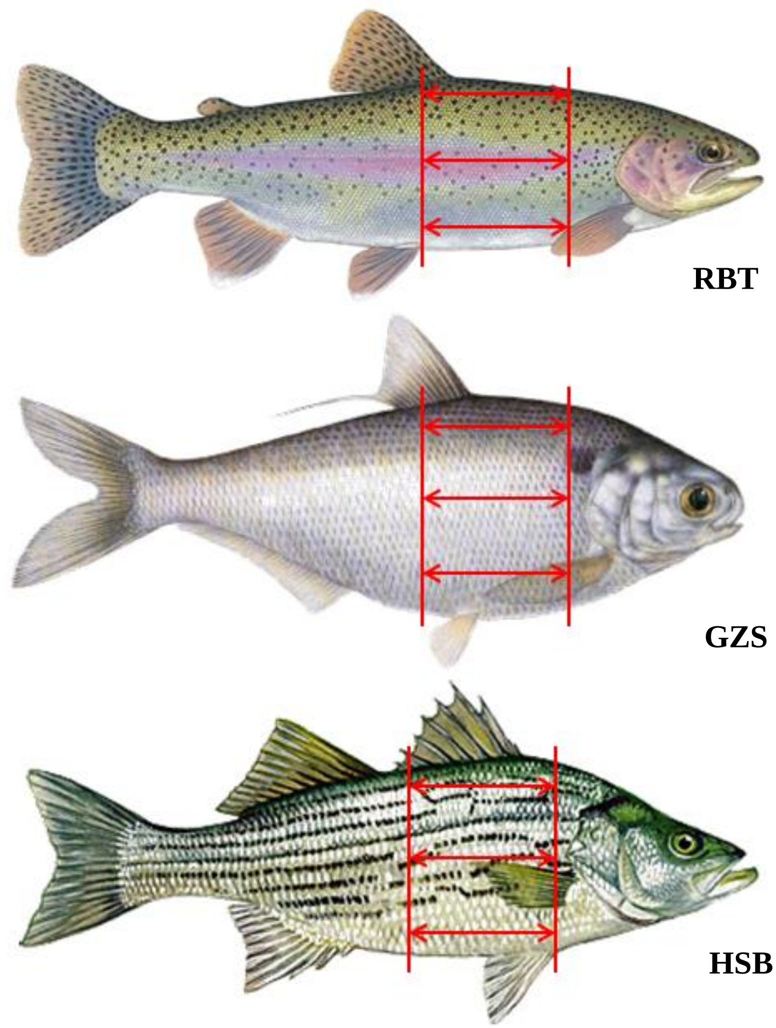

Figure 4. The figure above depicts the targeted exposure area (TEA; area between vertical lines) found on the dextral side of rainbow trout (RBT), gizzard shad (GZS), and hybrid striped bass (HSB) used to estimate scale loss. Scale loss was estimated by placing a 35 × 35 mm square (1225 mm2 surface area) within the TEA during post hoc image analyses. See text for more information related to nozzle alignment for each species.

Quantification of Scale Loss

Photography – Two digital SLR cameras were used to take pictures of fish before velocity exposure and after immersion in a fluorescein bath under Ultraviolet (UV) lighting. Pictures of fish before and after exposure velocity were taken with a tripod-mounted (Pentax model Optio 43WR) without flash to document the scale status of each fish before and after shear exposure. The second SLR digital camera (Canon model EOS T5i) was used to take pictures of fish following immersion in a fluorescein bath. One picture was taken at short (254 nm) and long (360 nm) wavelengths using a 6W UV lamp (UVGL Model 58) secured to the lid of photo booth and held ~30 cm above the surface of the fish. Two squares of known size (30 × 30 cm and 40 × 40 cm) were placed inside the booth as a scale reference for eventual image analysis to estimate scale loss. The UV photo booth was designed to block out all ambient lighting from the laboratory thereby ensuring pictures captured maximum fluorescence. Separate cameras were necessary to encourage efficient processing time, and so that International Organization of Standardization (ISO), aperture, and exposure time could be modified (i.e., 1600, f/4.5, and 1/2 sec., respectively) for UV photography.

Fluorescein Protocol – We estimated scale-loss by immersing every fish into a water bath of fluorescein dye which fluoresces under UV light when the dye interacts with damaged epithelial tissue (Colotelo et al., 2009). Each fish was placed into a 14-L water bath containing 0.2 mg/ml fluorescein (40% fluorescein sodium salt solution; density = 1.602 g/mL) for 6 minutes. After dye immersion, fish were rinsed twice, for 2 minutes in two separate tanks containing clean freshwater (Noga & Udomkusonsri, 2002; Colotelo & Cooke, 2011). The latter ensured excess dye was removed before UV photography to avoid overestimation of scale loss caused by accumulation of dye solution.

Exposure Procedure – Experiments exposing fishes to simulated shear velocities were accomplished by processing groups of 20 individuals of one species at a time. Individuals were removed from holding tanks with rubber coated nets to minimize scale loss during handling. Fish were euthanized in a 200 – 400 ppm solution of clove oil dissolved in 95% ethanol (1:9 mixture; Javahery et al., 2012). Clove oil was used instead of tricaine methanesulfonate (i.e., MS-222) to euthanize fish because MS-222 can cause direct damage to the epidermis and cornea of fish (Davis et al., 2008), potentially leading to an overestimate of scale-loss during simulated shear exposure experiments. Following euthanasia, each fish was randomly assigned a treatment (either control or exposure velocity) and secured onto the SERD as described previously. A unique numerical identifier was used for each fish within a given processing group to ensure accurate data entry. Two pictures were taken of each fish, before and after simulated shear exposure, prior to immersion in the fluorescein bath. After two rinses, fish were placed in the UV booth close to the scale reference and photographed at both UV wavelengths. Lastly, the total length (cm) of every each fish was recorded.

Image Analysis – ImageJ software (National Institute of Health, 2015) was used to quantify scale loss by analyzing the longwave UV photographs. Photographs were imported directly into the software and a 35 × 35 cm square within the TEA was created relative to the scaled reference using the software's specify prompt. Once the TEA was placed, all other areas of the fish were excluded so that descaling could be estimated within the square. Descaling was estimated by counting fluorescing pixels within the square using color threshold filters. More specifically, we used the hue color space which also includes saturation and brightness, all of which range from 0 – 255 and can be individually adjusted. The entire range of saturation and brightness were used in this analysis, but hue was adjusted so that only pixels within the 130 – 255 range would be counted. This range was chosen because pixel coverage for areas fluorescing under UV distinguished between scaled and descaled zones the best when compared with before and after photographs. Using this method, we determined total pixels and pixels within the square not fluorescing under longwave UV using the ImageJ's analyze feature. The proportion descaled was calculated using the following equation:

$$PD = \frac{(T_{pix} - ND_{pix})}{T_{pix}}, \qquad (1)$$

where PD is the proportion descaled and ranges from 0 – 1, T_{pix} is the total pixels, and ND_{pix} is pixels from areas not descaled within the TEA.

Data Analysis

Descaling data were analyzed using a traditional dose-response relationship where the dose (exposure velocity, m/s) was used to model the response (proportion of 35 × 35 square descaled) using logistic regression. Before analysis, group data were tested for outliers using the Modified Thompson Tau Outlier Test that identified two outliers from the 11.0 m/s exposure treatment for rainbow trout. Additionally, data for the highest exposure velocities were normalized to the individual with greatest descaling because we observed the 35 × 35 mm square was slightly larger than the TEA – i.e., individuals with the highest descaling were considered 100% descaled and all other values were normalized to this individual. Finally, data were analyzed using a four-parameter log-logistic model function according to the following equation described in Ritz et al., 2015:

$$f(x; b, c, d, e) = c + \frac{d-c}{1+\left(\frac{x}{e}\right)^{b}} \qquad (2)$$

where f(*x; b*, *c*, *d*, *e*) is the predicted proportion descaled when x is the exposure velocity (m/s), b is the slope, c is lowest value fixed at 0, d is the highest value fixed at 1, and e or E50 represents the exposure velocity at which 50% of the population would be descaled. Regression analyses and goodness of fit tests were performed using the drc-package for dose-response data in *R v3.4.21* (Ritz et al., 2015). All statistical decisions were based on a type I error rate of 5%.

3. RESULTS

Exposure to simulated shear forces had a clear effect on proportional scale loss for all species as exposure velocity increased. Furthermore, our system consistently induced scale loss that is qualitatively visible across the continuum of exposure velocities (Figure 5), and the fluorescein procedure allowed scale loss to be quantified consistently using UV photographs and color analysis with ImageJ software (Figure 6). The four-parameter log-logistic regression analyses produced models with significant parameter estimates (*b* and *e*, Table 1) for each species. Predicted models also fit our dose-response data well compared to fully parameterized models and one-way Analysis of Variance (ANOVA) on groups for each species (Table 2).

The models predict little to no descaling for shad until exposure velocity approached 3 m/s and for trout and bass about 5 m/s (Figure 7). Similarly, shad were predicted to experience 50% scale loss at 5.6 m/s compared to bass and trout at 6.5 and 9.5 m/s, respectively (Table 1). Trout were more resistant to scale loss at all velocities compared to shad and bass. Bass had the highest estimated slope among species tested indicating that small changes in exposure velocity led to proportionally higher scale loss as velocity neared 6.5 m/s. Both shad and bass curves behaved similarly at higher velocities where ~100% descaling was observed around 7.5 m/s. Trout, however, experienced only 25% descaling at 7.5 m/s and the mean scale loss of 75% was observed at 11.0 m/s; however, several of the trout experienced virtually 100% descaling at this velocity. The differences among species are evident in a graph depicting all three log-logistic curves, which had visibly different shapes, slopes, and position over the specified range of exposure velocities (Figure 7).

Figure 5. A single sample group of 20 hybrid striped bass exposed to either to a simulated shear jet of either 0, 4.3, 5.9, or 7.3 m/s. Descaled areas (X) on fish were identifiable prior to the fluorescein immersion bath, though this dye does make visual identification of descaling areas easier as seen here.

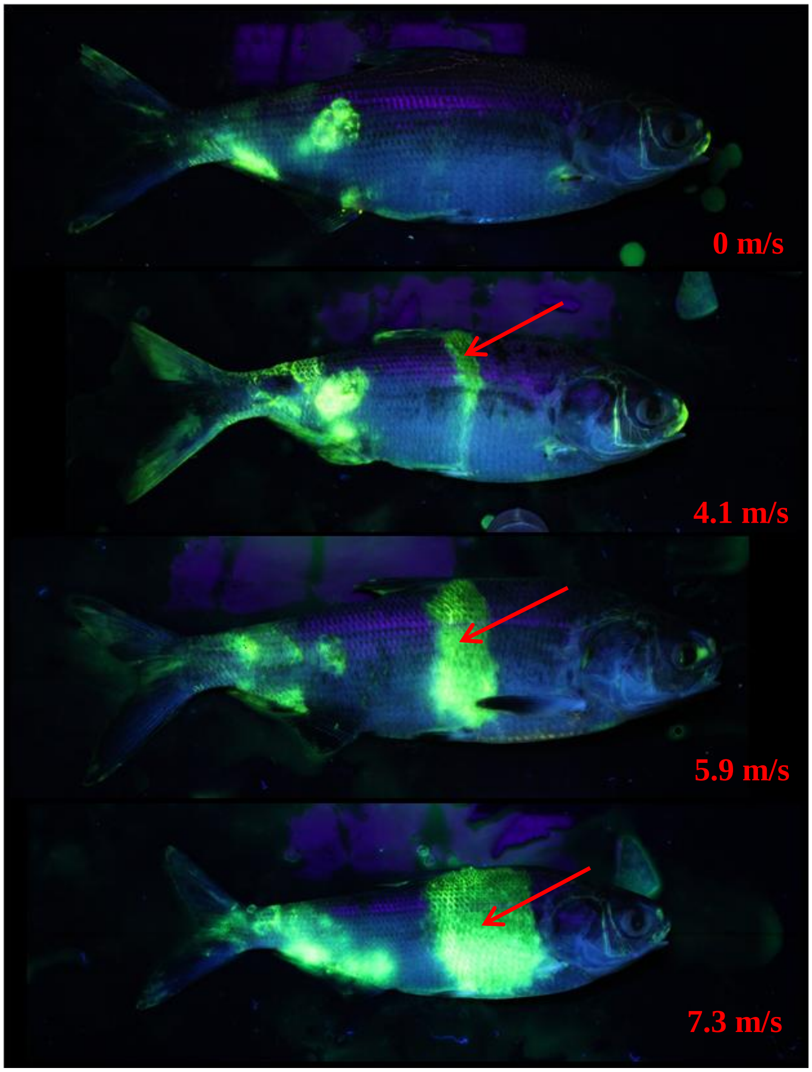

Figure 6. The fluorescein dye procedure allowed for consistent quantification of scale loss when combined with longwave UV photography (pictured above) and ImageJ analysis. The gizzard shad in this image show increased descaling trends within the targeted exposure area (red arrows) associated with increasing exposure velocity.

Table 1. The four-parameter log-logistic regression of proportion descaled versus exposure velocity (m/s) produced models with significant parameter estimates (*b* and *e*) for each species – rainbow trout (RBT), gizzard shad (GZS), and hybrid striped bass (HSB).

Species	P	PE	SE	p-value*
RBT	*b*	-5.51	0.646	<< 0.001
	e	9.54	0.183	<< 0.001
GZS	*b*	-6.22	0.649	<< 0.001
	e	5.65	0.099	<< 0.001
HSB	*b*	-12.98	0.672	<< 0.001
	e	6.51	0.035	<< 0.001

NOTE: Four total parameters (P) were tested with the model estimating "*b"* the slope where "*e"* represents the E50 value (i.e., exposure velocity causing 50% of the population to be descaled), whereas the lower limit *"c"* and upper limit *"d"* were fixed at 0 and 1, respectively. Actual parameter estimates (PE) are paired with standard error of the parameter estimates (SE). *Reported p-values for each parameter estimate were all considered highly significant (i.e., non-zero) according to $\alpha = 0.05$.

Table 2. Lack of fit tests suggest log-logistic regression models for rainbow trout (RBT), gizzard shad (GZS), and hybrid striped bass (HSB) described our dose-response better than the fully parameterized model and one-way ANOVA across exposure velocity treatments.

Species	n	Accepted Model Description	Lack of Fit Tests	
			Comparison Model	**p-value[1]**
RBT	121	LL.4 {c(0), d(1)}	LL.4 {full}	0.3066
			One-way ANOVA	0.3064
GZS	121	LL.4 {c(0), d(1)}	LL.4 {full}	0.3870
			One-way ANOVA	0.3869
HSB	122	LL.4 {c(0), d(1)}	LL.4 {full}	0.4288
			One-way ANOVA	0.4199

NOTE: Accepted models for each species correspond to four parameter log-logistic regression (LL.4[*]) where the lower limit *"c"* and upper limit *"d"* were fixed at 0 and 1, respectively. The latter models were compared to the same log-logistic regression model that estimated all four parameters (full; *b, c, d, e,* see Eqn. 2) and to a one-way ANOVA across groups to assess model fit. [1] P-values < 0.05 indicate the accepted model did not fit the data relative to either comparative model, whereas p-values > 0.05 indicate that (1) the accepted model fit the data as well as the fully parameterized model, and (2) the log-logistic regression model fit the data better than an ANOVA between groups. [*] This nomenclature is used in the *drc* package of *R v3.4.2* to represent the four parameter log-logistic function during dose-response model fitting.

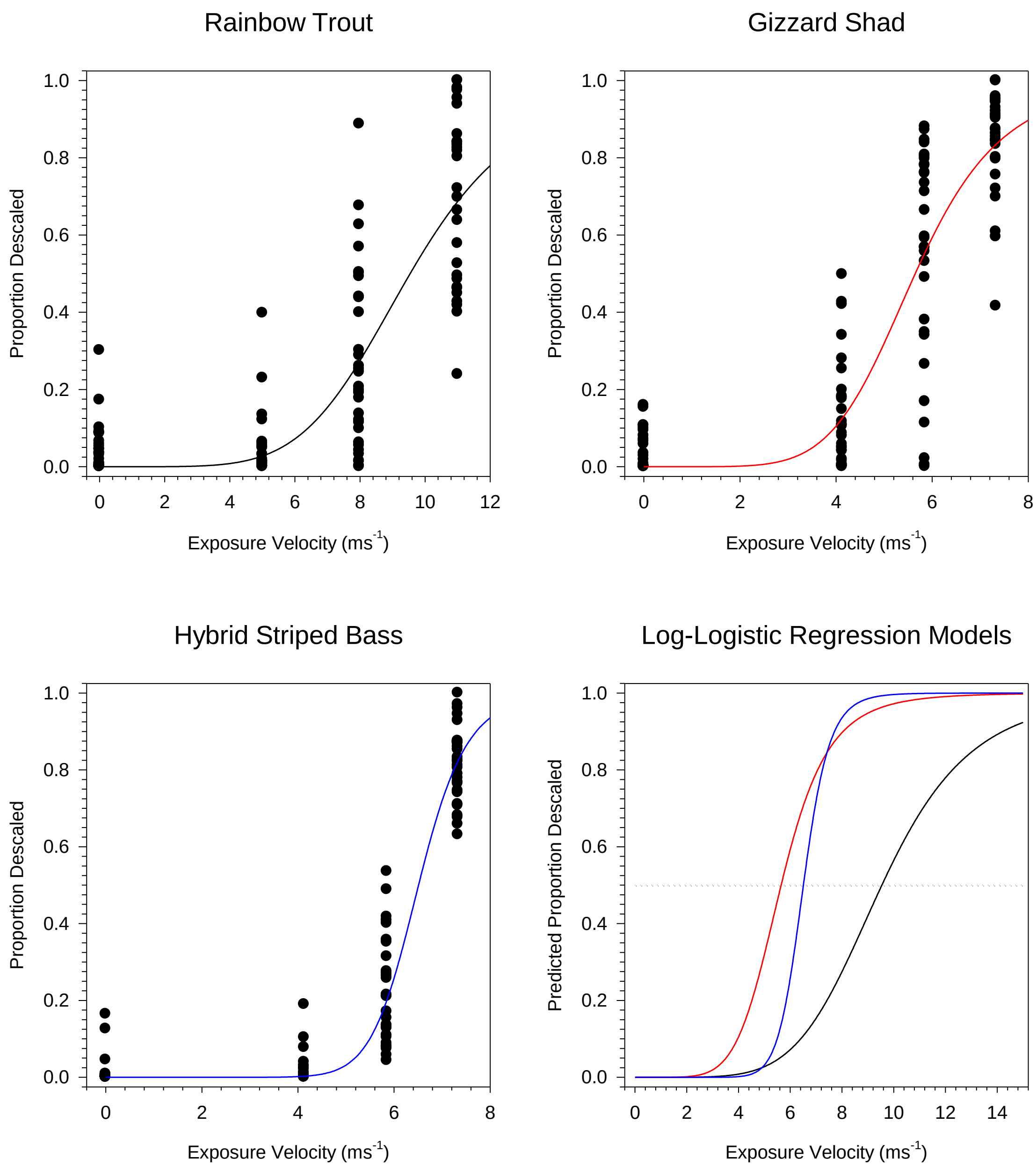

Figure 7. The graphs (1 – 3) above depict exposure velocity (m/s) versus proportion of the 35 × 35 cm square descaled for rainbow trout, gizzard shad, and hybrid striped bass. Graph (4) depicts exposure velocity (m/s) versus predicted proportion descaled according to the four parameter log-logistic regression models fit to rainbow trout (—), gizzard shad (—), and hybrid striped bass (—) shear data. The dotted line represents 50% descaling across all species and the intersection with each curve corresponds to the *"e"* or E50 parameter, i.e., the exposure velocity at which 50% of the population was predicted to be descaled.

4. DISCUSSION

Our shear exposure delivery system consistently caused scale loss for all species studied once exposure velocity increased above 3-5 m/s. The fluorescein dye procedure allowed for consistent estimation of descaling using longwave UV fluorescence and post-hoc image analysis. ImageJ software allowed us to precisely quantify scale loss using the hue color space to constrain color thresholds to only count fluorescing pixels. We are confident that our estimates reflect a dose and response because image software was not influenced by epidermal damage observed in photographs prior to exposure. Log-logistic regression fit the dose-response data well, with different models for each species. Species-specific differences in the fitted models likely reflect natural variation in scale size, number, overlap, and type among test species. One assumption of our data is that the estimated descaling reported here could be caused by shear water forces during passage through turbines, which was observed during field studies where fish with poorest condition also had the highest descaling rates (Basham et al., 1982).

We calculated strain rates (shear forces) following Neitzel et al. 2004 to compare our scale loss data to other shear studies. Our calculations also used average exposure velocity, but our test fish were stationary and did not move into a flow field as in the PNNL studies (Neitzel et al., 2004; Deng et al., 2005). Hence, the difference in velocity fields was calculated as the velocity at the exit of the jet (4.1 to 11.0 m/s) minus the speed of the fish (0 m/s). Perpendicular distance (relative to the flow field) was set to 1 cm representing the distance between the nozzle tip and body surface, whereas the Neitzel and Deng studies used 1.8 cm – the body width of the smallest fish. For comparison, we also calculated strain rates for 0.5 and 2.0 cm to highlight how choice of the perpendicular distance value influences strain rate calculations. Calculated strain rates were 410-1100 /s for a perpendicular distance of 1 cm (205 – 2200 /s across all velocities and perpendicular distances), which is within the range reported by previous studies (Table 3.). Rainbow trout experienced the greatest scale loss at a strain rate of 1100 /s, which is similar to Neitzel et al. (2004) who found major injuries (which included descaling) when strain rates exceeded 1008 /s. Both studies found that rainbow trout were more resistant to shear forces compared to the other species tested. In contrast, gizzard shad experienced higher scale loss at a lower strain rate (410 /s), which was also observed in American shad at strain rates < 400 /s by (Neitzel et al., 2004)). Further comparisons are problematic because we tested larger fish (> 18.0 cm TL) and the PNNL studies only reported that an injury occurred and did not separate descaling from other trauma (e.g., hemorrhaging, ocular removal, gill damage, etc.) in their injury assessments (Neitzel et al., 2004; Deng et al., 2005).

The log-logistic curves fit species dose-response data well but also indicate that descaling is species dependent. The shape of functional response curve (and overall dose-response relationship) is likely linked to scale type and size disparities among species (Figure 8). Rainbow trout have small, more densely compacted cycloid scales (Cockerell, 1911; Roberts, 1993) whose properties have been shown to change during spawning season. During experimentation, we noticed that scale loss in males with spawning characteristics (as indicated by kipe formation, darkened coloration, and excretion of milt) was noticeably different from other rainbow trout. We surmised these sexually dimorphic traits linked with innate spawning cues affected descaling estimates for these individuals, especially at 11.0 m/s. Histological changes do occur in male salmonids during spawning activities when dermal connective tissue thickens and scales become more deeply embedded in the skin of spawning males (Stoklosowa, 1970). In addition, spawning may also induce scale resorption of calcium causing "spawning scars" (Bruno et al., 2013) and may also explain why scale loss in these males was lower and more patchy. Gizzard shad and other Clupeids have cycloid scales that are deciduous (i.e., often lost and replaced), less imbricated (i.e., less scale overlap), and attached less securely to the skin causing scales to be lost easily (Lagler, 1947). Gizzard shad began losing scales at the lowest velocity of any test species (< 4 m/s), and 50% descaling occurred at 5.6 m/s compared to hybrid striped bass (6.5 m/s) tested over the same range of exposure velocities. Hybrid striped bass have ctenoid scales of similar size to that of gizzard shad, but have more imbrication (Lagler, 1947; Roberts, 1993), and the water jet might interact with ctenes on scale margins to make the bass more resistant to descaling. Future work should analyze which exposure levels are most important predictors of shear stressors, to prioritize research on more species to broaden our inference space and better parameterize the BioPA model.

Scale loss in fishes was a direct response to shear exposure at levels similar to turbine passage conditions; however, no singular explanation of how scale loss may affect mortality is available. Previous field and laboratory studies have suggested that scale loss plays a role in fish mortality during turbine passage, but none of these studies quantified how descaling may cause mortality, directly or indirectly, in fishes (Basham et al., 1982; Kostecki et al., 1987; Turnpenny, 1998; Neitzel et al., 2004; Deng et al., 2005). Estimated mortality rates of 60% in herring were found when at least 50% of their body surface was descaled (Olsen et al., 2012). The actual cause of mortality may be latent effects (i.e., days after scale loss) associated with poor fish condition, osmotic stress, and elevated stress response (Gadomski et al., 1994; Zydlewski et al., 2010; Olsen et al., 2012). The greatest impact to osmoregulation in Atlantic salmon smolts was observed up to 3 days after 10% of body surface was descaled (Gadomski et al., 1994; Zydlewski et al., 2010) which could be a factor of latent mortality after turbine passage. Increased susceptibility to diseases may also play a role due to loss of protective mucous and because of poor fish condition caused by chronic physiological stress associated with scale loss in fishes (Gadomski et al., 1994; Hostetter et al., 2011; Noble et al., 2012; Olsen et al., 2012). Physiological indicators of stress including blood osmolarity, cortisol, lactates, or glucose may be useful comparative metrics, but are currently underutilized in turbine passage research (Colotelo et al., 2017). Predation on descaled or stressed fish is also a possible cause of indirect mortality after turbine passage (Poe et al., 1991), but laboratory studies were unable to infer a significant relationship between descaling and increased predation (Gadomski et al., 1994). Risk of predation may still affect mortality after shear exposure experienced during turbine passage or interaction with turbulence in dam tail waters.

This study and others have shown that shear forces directly cause scale loss, but the following research is needed: (1) inclusion of additional species to broaden our understanding of the breadth of responses by species exposed to hydropower turbine passage, and (2) the relationship between descaling and latent health effects to better understand what rates of descaling are of concern with regards to population-level effects. Between the shear studies conducted at PNNL and ORNL only three of the seven taxonomic groups listed as priority species for hydropower in the BioDE Multi-Year Research Plan have been tested (Table 4). Additional data on other species is necessary to develop a complete dose-response continuum for the species of interest. At risk species and surrogates all have different scale types, sizes, shapes, and densities; therefore, dose-response data on these species would provide better parameterization and increase the inference space of the BioPA model. Although the BioPA can be modified to include probability of injury, which is the most likely immediate outcome of shear stress exposure, linking shear-induced injuries such as descaling to future probability of mortality would be more consistent with other dose-response relationships in the BioPA. Linking empirically derived dose-response data to latent mortality could be achieved by quantifying the relationship between physiological metrics like fish condition, physiological stress response, and disease susceptibility relative to scale loss. In addition, latent mortality caused by increased predation risk of descaled fishes would better quantify the population-level effects of scale loss on fishes following turbine passage.

Table 3. Calculated strain rates for this study are similar to those reported in shear studies by Neitzel et al. (2004) and Deng et al. (2006).

Velocity (m/s)	Calculated Strain Rates (/s) According to Exposure Distance (cm)				
	0.5[a]	1.0[a]	2.0[a]	1.8[b]	1.8[c]
3.0	--	--	--	166.7	166.7
4.1	820.0	410.0	205.0	--	--
5.0	1000.0	500.0	250.0	--	--
5.9	1180.0	590.0	295.0	--	--
6.1	--	--	--	338.9	--
7.3	1460.0	730.0	365.0	--	--
8.0	1600.0	800.0	400.0	--	--
9.1	--	--	--	505.5	--
11.0	2200.0	1100.0	550.0	--	--
12.2	--	--	--	677.8	677.8
13.7	--	--	--	--	--
15.2	--	--	--	844.4	844.4
16.8	--	--	--	--	933.3
18.3	--	--	--	1016.7	1016.7
19.8	--	--	--	--	1100.0
21.3	--	--	--	1183.3	--

NOTE: Strain rates are reported with units of (m/s/s or /s) and were calculated following Neitzel et al. 2004. Strain rates are reported for three studies: [a] this study, [b] Neitzel et al. 2004, and [c] Deng et al. 2006. See text body for more detailed description on exposure distance and how it was chosen during strain rate calculations.

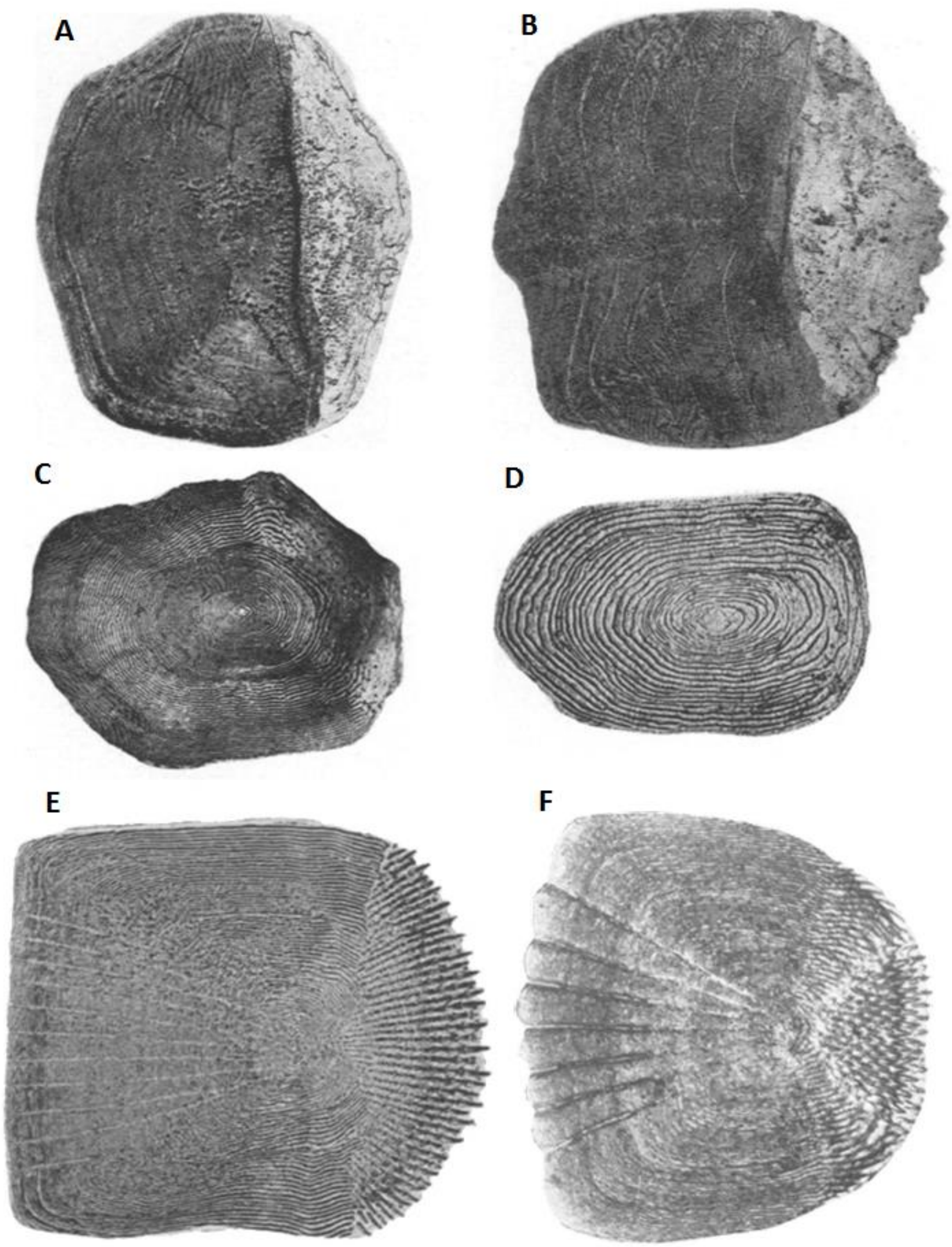

Figure 8. Representative fish scales from (A) gizzard shad, (B) American shad, (C) rainbow trout, (D) brook trout, (E) white bass, and (F) largemouth bass. Gizzard shad and rainbow trout were used in this study. White bass was included here as a substitute for hybrid striped bass. American shad, brook trout, and largemouth bass scales were included to show variation in scale shape, morphology, size, etc…for fishes that may be from the same family. Specifically, families include Clupeidae (A & B), Salmonidae (C & D), as well as Moronidae (E) and Centrarchidae (F). Images of scales were taken from Lagler 1947.

Table 4. Summary of priority species and life stages for the BioDE dose-response studies. This is a working document produced by traits-based analysis and expert opinion of team members participating in this research at ORNL. (Source: the 2017 BioDE Multi-Year Research Plan)

Species Group	Species	Life Stages	Region	Justification	Proposed Surrogate Species
Family Salmonidae	Steelhead	Juv&Adult	PNW	Listed under ESA	Rainbow trout
	Bull trout	Juv&Adult	PNW	Listed under ESA	Brook trout, lake trout
	Atlantic salmon	Juv&Adult	East Coast (Gulf of Maine)	Listed under ESA	None
Family Clupeidae	American shad	Juv&Adult	Atlantic coast	Listed under ESA	Gizzard shad
	Blueback herring	Juv&Adult	Atlantic coast	Listed under ESA	Gizzard shad American shad
	Alewife		Atlantic coast	Species of Concern for NOAA	Gizzard shad American shad
Family Centrarchidae	Largemouth bass	Juv&Adult	All	Commonly found throughout US; popular gamefish	Bluegill
	Smallmouth bass	Juv&Adult	All	Commonly found throughout US; popular gamefish	Bluegill
	Bluegill*	Adult	All	Commonly found in US; Physoclistous	*Lepomis* spp.
Order Perciformes	Yellow Perch*	Juv&Adult	All	Commonly found throughout US; Physoclistous (closed swim bladder)	None
	Walleye	Juv&Adult	North and Midwest	Commonly throughout US; popular gamefish	None
	Sauger	All	All	Commonly found throughout US; popular gamefish; migratory	None
	Striped bass	Larvae Adult	Atlantic coast U.S.	Downstream drifting larvae; popular gamefish	Hybrid striped bass White bass
Order Cypriniformes	Blue sucker	Adult	Miss. and Missouri rivers	Migratory	Common sucker, redhorse sucker
	White sucker	Adult	Midwest, NE, South	Commonly found throughout US	
Order Acipen-seriformes	Sturgeon (All species)	Larvae Juvenile Adult	All	Conservation concern/listed under ESA; popular gamefish; downstream drifting larvae	Lake sturgeon
	Paddlefish	Larvae Juvenile Adult	Mississippi River Basin	Conservation concern/listed under ESA; popular gamefish; downstream drifting larvae	None
Order Anguillidae	American eel	Adult	Atlantic and Gulf coast	Conservation concern; downstream migrating adults	None

5. REFERENCES

Basham, L. R., M. R. Delarm, J. B. Athearn, & S. W. Pettit, 1982. Transport Operations on the Snake and Columbia Rivers. .

Bruno, D., P. Noguera, & T. Poppe, 2013. Chapter 2: Functional Anatomy A Colour Atlas of Salmonid Diseases. Springer Dordrecht Heidelberg, New York: 5–26.

Čada, G. F., 1998. Fish Passage Mitigation at Hydroelectric power Projects in the United States In Jungwirth, Mathias; Schmutz, Stefan; & Weiss, S. (ed), Fish Migration and Fish Bypasses. Fishing New Books, Malden, Massachusetts: 208–219.

Čada, G. F., 2001. The development of advanced hydroelectric turbines to improve fish passage survival. Fisheries 26: 14–23.

Čada, G. F., & P. E. Schweizer, 2012. The Application of Traits-Based Assessment Approaches to Estimate the Effects of Hydroelectric Turbine Passage on Fish Populations. Oak ridge, Tennessee.

Čada, G., J. Loar, L. Garrison, R. Fisher, & D. Neitzel, 2006. Efforts to Reduce Mortality to Hydroelectric Turbine-Passed Fish: Locating and Quantifying Damaging Shear Stresses. Environmental Managment 37: 898–906.

Cockerell, T. D. A., 1911. The Scales of Freshwater Fishes. Biological Bulletin 20: 367–387.

Colotelo, A. H., & S. J. Cooke, 2011. Evaluation of common angling-induced sources of epithelial damage for popular freshwater sport fish using fluorescein. Fisheries Research 109: 217–224.
Colotelo, A. H., S. J. Cooke, & K. E. Smokorowski, 2009. Application of forensic techniques to enhance fish conservation and management: injury detection using presumptive tests for blood. Endangered Species Research 9: 169–178.

Colotelo, A. H., A. E. Goldman, K. A. Wagner, R. S. Brown, Z. D. Deng, & M. C. Richmond, 2017. A comparison of metrics to evaluate the effects of hydro-facility passage stressors on fish. Environmental Reviews 25: 1–11.

Davis, M. W., J. Stephenson, & E. J. Noga, 2008. The Effect of Tricaine on Use of the Fluorescein Test for Detecting Skin and Corneal Ulcers in Fish. Journal of Aquatic Animal Health 20: 86–95, http://www.tandfonline.com/loi/uahh20.

Deng, Z., G. R. Guensch, C. a McKinstry, R. P. Mueller, D. D. Dauble, & M. C. Richmond, 2005. Evaluation of fish-injury mechanisms during exposure to turbulent shear flow. Canadian Journal of Fisheries and Aquatic Sciences 62: 1513–1522.

Gadomski, D. M., M. G. Mesa, & T. M. Olson, 1994. Vulnerability to predation and physiological stress responses of experimentally descaled juvenile chinook salmon , Oncorhynchus tsha wytscha. Environmental Biology of Fishes .

Hostetter, N. J., a. F. Evans, D. D. Roby, K. Collis, M. Hawbecker, B. P. Sandford, D. E. Thompson, & F. J. Loge, 2011. Relationship of External Fish Condition to Pathogen Prevalence and Out-Migration Survival in Juvenile Steelhead. Transactions of the American Fisheries Society 140: 1158–1171.

Hydropower Explained: Energy from moving water. , 2017.USEIA. U.S. Energy Information Administration, Washington, D.C.

Javahery, S., H. Nekoubin, & A. H. Moradlu, 2012. Effect of anaesthesia with clove oil in fish (review). Fish Physiology and Biochemistry 38: 1545–1552.

Kostecki, P. T., P. Clifford, S. P. Gloss, & J. C. Carlisle, 1987. Scale Loss and Survival in Smolts of Atlantic Salmon (Salmo salar) after Turbine Passage. Canadian Journal of Fisheries and Aquatic Sciences 44: 51–52.

Lagler, K. F., 1947. Lepidological Studies 1. Scale Characters of the Families of Great Lakes Fishes. Transactions of the American Fisheries Society 66: 149–171.

Neitzel, D. A., M. C. Richmond, D. D. Dauble, R. P. Mueller, R. A. Moursund, C. S. Abernethy, G. R. Guensch, & G. F. Cada, 2000. Laboratory Studies on the Effects of Shear on Fish. Richland, Washington.

Neitzel, D. a, D. D. Dauble, G. F. Cada, M. C. Richmond, G. R. Guensch, R. R. Mueller, C. S. Abernethy, & B. Amidan, 2004. Survival estimates for juvenile fish subjected to a laboratory-generated shear environment. Transactions of the American Fisheries Society 133: 447–454.

Noble, C., H. A. C. Jones, B. Damsgard, M. J. Flood, K. O. Midling, A. Roque, B.-S. Saether, & S. Y. Cottee, 2012. Injuries and deformities in fish: Their potential impacts upon aquacultural production and welfare. Fish Physiology and Biochemistry 38: 61–83.

Noga, E. J., & P. Udomkusonsri, 2002. Fluorescein: A Rapid, Sensitive, Nonlethal Method for Detecting Skin Ulceration in Fish. Vet Pathol 39: 726–731.

Normandeau, A., J. R. Skalski, & M. C. Consulting, 1996. Fish survival investigation relative to turbine rehabilitation at Wanapum Dam, Columbia River, Washington. Ephrata, Washington.

Olsen, R. E., F. Oppedal, M. Tenningen, & A. Vold, 2012. Physiological response and mortality caused by scale loss in Atlantic herring. Fisheries Research 129–130: 21–27.

Poe, T. P., H. A. L. C. Hansel, S. Vigg, D. E. Palmer, & L. A. Prendergast, 1991. Feeding of Predaceous Fishes on Out-Migrating Juvenile Salmonids in John Day Reservoir, Columbia River. Transactions of the American Fisheries Society 120: 405–420.

Pracheil, B. M., C. R. DeRolph, M. P. Schramm, & M. S. Bevelhimer, 2016a. A fish-eye view of riverine hydropower systems: the current understanding of the biological response to turbine passage. Reviews in Fish Biology and Fisheries Springer International Publishing 26: 153–167.

Pracheil, B. M., R. A. McManamay, M. S. Bevelhimer, C. R. DeRolph, & G. F. Čada, 2016b. A traits-based approach for prioritizing species for monitoring and surrogacy selection. Endangered Species Research 31: 243–258.

Ritz, C., F. Baty, J. C. Streibig, & D. Gerhard, 2015. Dose-response analysis using R. PLoS ONE 10: 1–13.

Roberts, C. D., 1993. Comparative Morphology of Spined Scales and Their Phylogenetic Significance in the Teleostei. Bulletin of Marine Science 52: 60–113.

Stoklosowa, S., 1970. Further observations on the sexual dimorphism in the skin of Salmo trutta trutta in relation to sexual maturity. Copeia 1970: 332–339, http://www.jstor.org/stable/1441655.

Turnpenny, A. W. H., 1998. Mechanisms of Fish Damage in Low Head Turbines: An Experimental Appraisal Fish migration and fish bypasses. : 300–314, http://scholarworks.umass.edu/fishpassage_book_chapters/18%5Cnhttp://scholarworks.umass.edu/fishpassage_book_chapters/18/.

van Esch, B. P. M., I. L. Y. Spierts, & K. Tierney, 2014. Validation of a model to predict fish passage mortality in pumping stations. Canadian Journal of Fisheries and Aquatic Sciences 71: 1910–1923.

Zydlewski, J., G. Zydlewski, & G. R. Danner, 2010. Descaling Injury Impairs the Osmoregulatory Ability of Atlantic Salmon Smolts Entering Seawater. Transactions of the American Fisheries Society 139: 129–136.